Austin Orthopedics

Open Access

Austin Publishing Group

Research Article

The Finite Element Analysis of Four Kinds of Pedicle Screw Internal Fixation in Different Osteoporosis

Wendong Xie[2]; Binbin AN[3]; Guangsu Zhang[2]; Chao Zhang[1*]

[1]Department of Orthopedics, Gansu Provincial Hospital, PR China

[2]Gansu University of Chinese Medicine, PR China

[3]Gansu Maternal and Child Healthcare Hospital, PR China

***Corresponding author: Chao Zhang**

Orthopedics Department, Gansu Provincial Hospital, No.204, Donggang West Road, Lanzhou, 730000, Gansu Province, PR China.

Email: zc-315@163.com

Received: July 30, 2024

Accepted: August 22, 2024

Published: August 29, 2024

Abstract

The aging society is serious, which leads to a significant increase in the incidence of bone metabolic diseases in senile osteoporosis. However, the screw loosening, extraction and non-fusion of bone graft caused by osteoporosis pose great challenges to clinicians. Therefor In this study, finite element analysis was used to evaluate the mechanical properties of four kinds of pedicle screw internal fixation in the treatment of different osteoporosis, so as to provide mechanical theoretical basis for biomechanical experiments and clinical experiments in the future.

Keywords: Osteoporosis; Spine; Pedicle screws; Internal fixation; Finite element analysis

Introduction

At present, China has entered an aging society. Senile osteoporosis is an age-related bone metabolic disease, and its incidence increases significantly with age [1]. In 2016, the prevalence of osteoporosis was as high as 36% in the elderly over 60 years old in China, with 23% in men and 9% in women [2]. The common spinal diseases in the elderly, such as lumbar spinal stenosis, degenerative lumbar spondylolisthesis, degenerative scoliosis, spinal fracture and so on, are often combined with osteoporosis, and the problems caused by osteoporosis, such as screw loosening, extraction, and non-fusion of bone grafting, bring great challenges to clinicians. With the rapid development of medical technology, take effective measures to prevent treatment for spinal diseases have become the focus in the field of spine surgery [3]. In recent years, with the rapid development of computer-aided imaging technology, it has played an important role in the prevention and clinical treatment of spinal diseases. Computer-aided imaging technology can ensure that doctors can complete the placement of spinal pedicle screws under direct vision, which can effectively improve the clinical treatment effect and promote the early recovery of patients [4].

Finite element analysis has been widely used in the biomechanical evaluation of spinal fractures, which can provide a basis for the selection of internal fixation methods for spinal fractures. The finite element model can be used to study the stiffness of spinal elements and the long-term effect of scoliosis correction, which has the advantages that in vivo experiments do not have [5]. In the process of establishing the model, the geometric morphology of the vertebral body and soft tissue can be obtained, and the corresponding biomechanical properties of each mechanism of the spinal segment can be assigned. The effectiveness and accuracy of the model are verified by comparing with the results of in vitro mechanical experiments. Studies have shown that the finite element model of spinal motion element is closely related to the type of each structural element to a certain extent, while relevant scholars believe that the finite element model can select a variety of material properties for different combinations, so as to select the best matching method [6]. However, when using finite element to simulate spinal pedicle screw placement in relevant studies, the results are more at the virtual level of software, and the results are obviously different from the actual situation. In addition, there is still a lack of unified standards for spinal stability reconstruction technology [7].

According to the orthopedics Department of Gansu Provincial People's Hospital, the finite element model was established by taking normal adult CT scan data through regular way. It is intended to analyze the application of different pedicle screws (Ordinary pedicle screw, Double thread pedicle screw, Cortical

Citation: Xie W, Binbin AN, Zhang G, Zhang C. The Finite Element Analysis of Four Kinds of Pedicle Screw Internal Fixation in Different Osteoporosis. Austin Orthop. 2024; 8(1): 1024.

bone trajectory screw and Expansion pedicle screw) in different osteoporosis patients (normal bone mass, osteopenia, osteoporosis, severe osteoporosis) by finite element analysis method to guide the clinical application of pedicle screw.

Materials and Methods

CT Data Sources

The CT data of normal adults in the Department of Orthopedics, Gansu Provincial People's Hospital were selected, and the 3D CT data were available and had sufficient definition.

The Establishment of the Finite Element Model

The CT images of the thoracolumbar spine were imported into the three-dimensional reconstruction software Mimics 21.0 (Materialise, Belgium) in DICOM format, and the three vertebral models of T12, L1 and L2 were reconstructed. The STL file format was imported into Geomagic 2021 (Geomagic, USA) for surface optimization and surface fitting to construct the vertebral model (Figure 1). A 3D model of the pedicle screw system was created using SolidWorks 2021 (Dassault, France) (Figure 2), and the pedicle screw system and the vertebral body model were assembled. Four fixation models and post-assembly models of the pedicle screw rod system were constructed (Figure 3). The bone and intervertebral disc were reticulated into a tetrahedral mesh, and the mesh size was selected as 1mm. The Ordinary Pedicle Screws (OPS) assembly has 636,633 nodes and 386,140 elements, the double-threaded Pedicle Screw (DPS) assembly has 645,492 nodes and 39,907 elements, and the cortical bone track screw (CBS) assembly has 650,339 nodes and 392,798 elements. The Expandable Pedicle Screw (EPS) assembly has 787,323 nodes and 491,669 elements. The assembled solid model was imported into the ANSYS Workbench 18.0 (ANSYS Corporation, USA) software for Boolean operation analysis. The units and nodes of the model are shown in Table 1.

Table 1: The unit and nodes of the model.

Model	OPS	DPS	CBS	EPS
nodes	636633	645492	650339	787323
unit	386140	390907	392798	491669

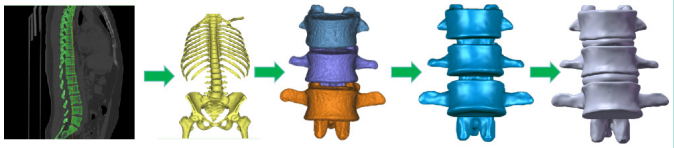

Figure 1: The establishment of the vertebral body model.

Table 2: Tensile longitudinal stiffness parameters of the ligament.

Name of Spring Ligament	Elastic Behavior	Longitudinal Stiffness (N/mm)
Anterior longitudinal ligament	Stretch	8.74
Posterior longitudinal ligament	Stretch	5.83
Intertransverse ligament	Stretch	2.39
Ligamenta interspinalis	Stretch	0.19
Ligamenta spinosum superior	Stretch	15.38
Ligamenta flavum	Stretch	15.75

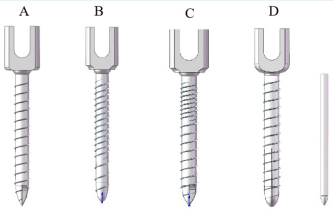

Figure 2: The 3D model of the pedicle screw system. A: Ordinary pedicle screws (5.5mm); B: Double-threaded pedicle screw (5.5mm); C: Cortical bone trajectory screw (5.5mm); D: Expandable pedicle screw (6 mm).

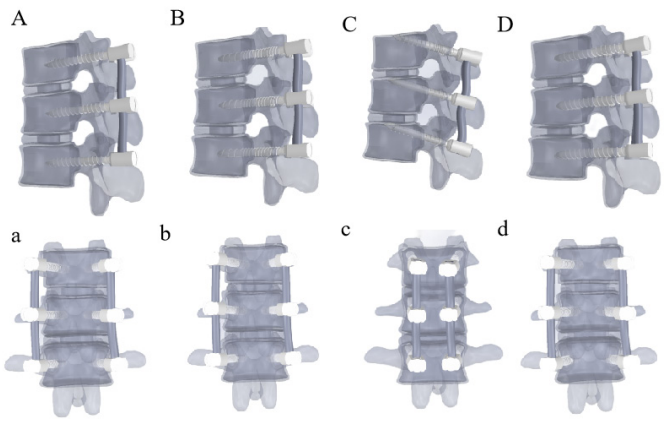

Figure 3: Four fixed assembly models: A: Ordinary pedicle screw assembly; B: Double-threaded pedicle screw assembly; C: Cortical bone track screw assembly; D: Expansion pedicle screw assembly.

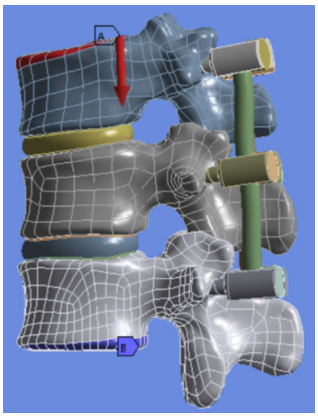

Figure 4: Four kinds of model of fixed constraint and load, A: force (500 N); B: Fixed support.

Material Properties, Boundary Conditions and Loads

According to the attachment position, the spring ligament is set to replace the solid ligament. The ligament parameters are shown in Table 2 below, and the elastic properties and Poisson's ratio of various structural materials are shown in Table 3. The interface between the screw and bone is set to be bonded. The cortical and cancellous bone are combined. The vertebral body is combined with the adjacent disc. The nucleus pulposus and annulus fibrosus are joined together, and the facet joint contact is set to a friction contact with a friction coefficient of 0.2. In order to mimic human lumbar true stress, under the surface of L2 completely fixed [8]. A load of 500N (perpendicular to the restraint surface) was applied to the upper surface of the first vertebral body T12 of the four groups of models, as shown in Figure 4.

The Evaluation Index

The four screw models were respectively implanted with normal bone (cortical bone 100%, cancellous bone 100%), osteopenia (cortical bone 85%, cancellous bone 85%), mild osteoporosis (cortical bone 75%, cancellous bone 65%), and severe osteoporosis (cortical bone 65%, cancellous bone 35%) with proportionally reduced elastic modulus. The internal fixation stress value and vertebral displacement value of four screw models in different bone were analyzed.

Results

The Comparison of Stress and Displacement of Internal Fixation System in Normal Bone

In normal bone (cortical bone 100%, cancellous bone 100%), the maximum stresses of OPS, DPS, CBS and EPS were 170.82

Table 3: Material properties used in finite element models.

Material Name	Elastic Modulus (Mpa)	Poisson Ratio
Cortical bone (normal)	12000	0.3
Cortical bone (85% osteopenia)	102	0.3
Cortical bone (mild osteoporosis 75%)	90	0.3
Cortical bone (severe osteoporosis 65%)	78	0.3
Cancellous bone (normal)	150	0.3
Cancellous bone (85% osteopenia)	127.5	0.3
Cancellous bone (mild osteoporosis 65%)	97.5	0.3
Cancellous bone (75% severe osteoporosis)	52.5	0.3
End plate	1000	0.4
Fibrous ring	4.2	0.45
Nucleus pulposus	1	0.49
Gristle	10	0.35
Nail bar	110000	0.28

Table 4: The comparison of stress and displacement of internal fixation system in normal bone.

Normal Bone	OPS	DPS	CBS	EPS
Maximum stress of nail rod (Mpa)	170.82	166.59	176.69	164.54
Maximum displacement of nail rod (mm)	1.1312	1.1055	1.3325	1.0395
Maximum body stress (Mpa)	28.86	27.41	36.42	24.78
Maximum vertebral displacement (mm)	1.4521	1.415	1.4700	1.3364

Mpa, 166.59 Mpa, 176.69 Mpa and 164.54 Mpa, respectively. The maximum displacements of screw rod were 1.312 mm, 1.1055 mm, 1.3325 mm and 1.0395 mm, respectively. The maximum stresses of vertebral body were 28.86 Mpa, 27.41 Mpa, 36.42 Mpa and 24.78 Mpa, respectively. The maximum displacements were 1.4521 mm, 1.4150 mm, 1.4700 mm and 1.3364 mm, respectively. Among them, CBS had the highest screw rod maximum stress, maximum displacement, maximum vertebral body stress, and maximum vertebral body displacement, while EPS had the lowest maximum stress and maximum displacement, as shown in Table 4.

The stress distribution cloud diagram of the screw showed that the stress distribution of the screw rod of OPS and CBS model was relatively concentrated, mainly concentrated in the roots of the two lower fixed screws and the cross-linked rod (Fig. 5A and C). The stress distribution of the screw rod of the DPS and EPS model was relatively scattered, and the two screws fixed below shared part of the stress, and the stress distribution on the whole rod was relatively uniform (Figure 5B & D). The distribution cloud diagram of screw displacement showed that the displacement of OSP and DPS models mainly occurred at the top of the two screws fixed above, the root of the screw and the cross-linked rod (Figure 5E & F). The displacement of the CBS and EPS models occurred mainly at the top of the two screws fixed above (Figure 5G & H).

The stress distribution cloud map of the vertebral body showed that the stress was mainly concentrated in the lower endplate and the middle column. Compared with the stress distribution transmitted to the upper endplate, the stress distribution in the upper endplate of the OPS, DPS, and EPS models was dispersed (Figure 6A,B, & D), and the stress distribution in the upper endplate of the CBS model was concentrated (Figure 6C). The distribution cloud map of vertebral body displacement showed that vertebral body displacement occurred at the upper endplate (Figure 6E,F,G & H).

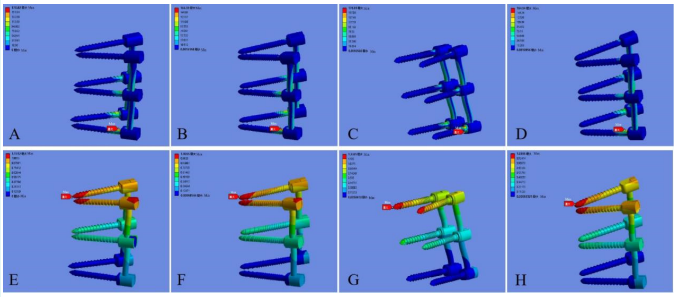

Figure 5: The nephogram of stress and displacement of posterior screws in normal bone pedicle nails, A: The stress nephogram of the Ordinary Pedicle Screws (OPS) model screw; B: The stress nephogram of the Double-threaded Pedicle Screw (DPS) model screw; C: The stress nephogram of the Cortical Bone track Screw (CBS) model screw; D: The stress nephogram of the Expansive Pedicle Screw (EPS) model screw; E: The displacement cloud image of the Ordinary Pedicle Screws (OPS) model screw; F: The displacement cloud image of the Double-threaded Pedicle Screw (DPS) model screw; G: The displacement cloud image of the Cortical Bone track Screw (CBS) model screw; H: The displacement cloud image of the Expansive Pedicle Screw (EPS) model screw.

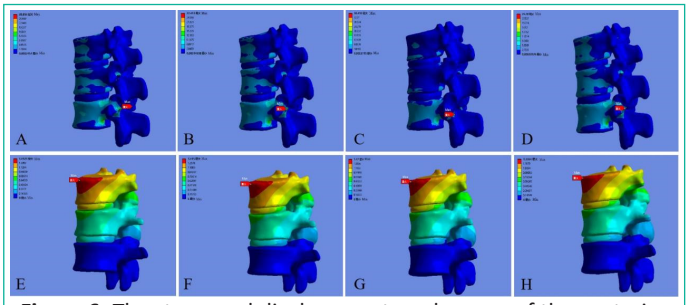

Figure 6: The stress and displacement nephogram of the posterior vertebral body of the pedicle nail in normal bone, A: The stress cloud image of the Ordinary Pedicle Screws (OPS) model vertebral body; B: The stress cloud image of the Double-threaded Pedicle Screw (DPS) model vertebral body; C: The stress cloud image of the Cortical Bone track Screw (CBS) model vertebral body; D: The stress cloud image of the Expansive Pedicle Screw (EPS) model vertebral body; E: The displacement cloud image of the Ordinary Pedicle Screws (OPS) model vertebral body; F: The displacement cloud image of the Double-threaded Pedicle Screw (DPS) model vertebral body; G: The displacement cloud image of the Cortical Bone track Screw (CBS) model vertebral body; H: The displacement cloud image of the Expansive Pedicle Screw (EPS) model vertebral body.

The Comparison of Stress and Displacement Reduction in Bone Fixation Systems

In reduced bone (cortical bone 85%, cancellous bone 85%), the maximum stresses of OPS, DPS, CBS and EPS were 167.21 Mpa, 163.28 Mpa, 172.95 Mpa, and 160.89 Mpa, respectively. The maximum displacements of the screw rod were 1.1626 mm, 1.1357 mm, 1.3689 mm and 1.0811 mm, respectively. The maximum stresses of vertebral body were 26.79 Mpa, 224.53 Mpa, 33.90 Mpa and 22.65 Mpa, respectively. The maximum vertebral displacements were 1.4927 mm, 1.4536 mm, 1.5072 mm and 1.3883 mm, respectively. Among them, CBS had the highest screw rod maximum stress, maximum displacement, maximum vertebral body stress, and maximum vertebral body displacement, while EPS had the lowest maximum stress and maximum displacement, as shown in Table 5.

Table 5: The reduce the stress and displacement of the internal fixation system in bone.

Osteopenia	OPS	DPS	CBS	EPS
Maximum stress of nail rod (Mpa)	167.21	163.28	172.95	160.89
Maximum displacement of nail rod (mm)	1.1626	1.1357	1.3689	1.0811
Maximum body stress (Mpa)	26.79	24.53	33.90	22.65
Maximum vertebral displacement (mm)	1.4927	1.4536	1.5072	1.3883

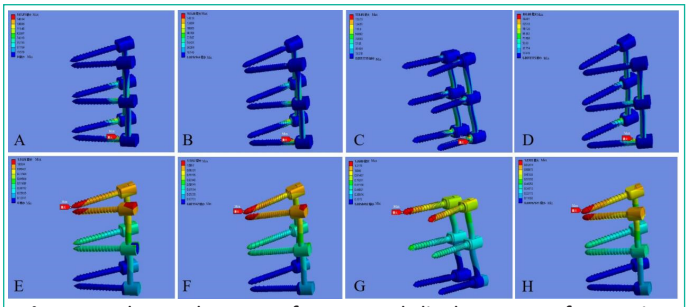

Figure 7: The nephogram of stress and displacement of posterior screws in bone fixation systems pedicle nails, A: The stress nephogram of the Ordinary Pedicle Screws (OPS) model screw; B: The stress nephogram of the Double-threaded Pedicle Screw (DPS) model screw; C: The stress nephogram of the Cortical Bone track Screw (CBS) model screw; D: The stress nephogram of the Expansive Pedicle Screw (EPS) model screw; E: The displacement cloud image of the Ordinary Pedicle Screws (OPS) model screw; F: The displacement cloud image of the Double-threaded Pedicle Screw (DPS) model screw; G: The displacement cloud image of the Cortical Bone track Screw (CBS) model screw; H: The displacement cloud image of the Expansive Pedicle Screw (EPS) model screw.

Table 6: The comparison of stress and displacement of internal fixation system in mild osteoporosis.

Mild Osteoporosis	OPS	DPS	CBS	EPS
Maximum stress of nail rod (Mpa)	166.07	162.37	170.84	159.75
Maximum displacement of nail rod (mm)	1.2064	1.1783	1.4150	1.1335
Maximum body stress (Mpa)	25.71	22.69	32.11	21.31
Maximum vertebral displacement (mm)	1.5488	1.5075	1.5555	1.4538

The stress distribution cloud diagram of the screw showed that the stress distribution of the screw rod of the CBS model was relatively concentrated, mainly concentrated in the roots of the two fixed screws below and the cross-linked rod (Figure 7C).The stress distribution of the screw rod of the OPS, DPS, and EPS model was relatively scattered, and the two screws fixed below shared part of the stress, and the stress distribution on the whole rod was relatively uniform (Figure 7A,B, & D).The distribution cloud diagram of screw displacement showed that the displacement of OPS and DPS models mainly occurred at the top of the two screws fixed above, the root of the screw and the cross-linked rod (Figure 7E & F).The displacement of the CBS and EPS models occurred mainly at the top of the two screws fixed above (Figure 7G & H).

The stress distribution cloud map of the vertebral body showed that the stress was mainly concentrated in the lower endplate and the middle column. Compared with the stress distribution transmitted to the upper endplate, the stress distribution in the upper endplate of the OPS, DPS, and EPS models was dispersed (Figure 8A,B, & D), and the stress distribution in the upper endplate of the cortical bone trajectory screw model was concentrated (Figure 8C). The distribution cloud map of vertebral body displacement showed that vertebral body displacement occurred at the upper endplate (Figure 8E,F,G & H).

The Comparison of Stress and Displacement of Internal Fixation System in Mild osteoporosis

In mild osteoporosis group (cortical bone 75%, cancellous bone 65%), the maximum stresses of OPS, DPS, CBS and EPS were 166.07 Mpa, 162.37 Mpa, 170.84 Mpa and 159.75 Mpa, respectively. The maximum displacements of screw rod were 1.2064 mm, 1.1783 mm, 1.4150 mm and 1.1335 mm, respectively. The maximum stresses of vertebral body were 25.71 Mpa, 22.69 Mpa, 32.11 Mpa and 21.31 Mpa, respectively. The maximum vertebral displacements were 1.5488 mm, 1.5075 mm, 1.5555 mm and 1.4538 mm, respectively. Among them, CBS had the highest screw rod maximum stress, maximum displacement, maximum vertebral body stress, and maximum vertebral body displacement, while EPS had the lowest maximum stress and maximum displacement, as shown in Table 6.

The stress distribution cloud diagram of the screw showed that the stress distribution of the screw rod of the OPS and CBS model was relatively concentrated, mainly concentrated in the roots of the two lower fixed screws and the cross-linked rod (Figure 9A & C).The stress distribution of the screw rod of the DPS model and the EPS model was relatively scattered, and the two screws fixed below shared part of the stress, and the stress distribution on the whole rod was relatively uniform (Figure 9B & D). The distribution cloud diagram of screw displacement showed that the displacement of OPS, DPS, and EPS models mainly occurred at the top of the two screws fixed above, the root of the screw, and the cross-linked rod (Figure 9E,F & H). The displacement of the CBS model occurred mainly at the top of the two screws fixed above (Figure 9G).

The stress distribution cloud map of the vertebral body showed that the stress was mainly concentrated in the lower end plate and the middle column. Compared with the stress distribution transmitted to the upper end plate, the stress distribution of the upper end plate in the OPS, DPS, and EPS models was dispersed (Figure 10A,B, & D). Cortical bone trajectory model of screw end plate on the stress distribution of the concentration (Figure 10C). The distribution cloud map of vertebral body displacement showed that vertebral body displacement occurred at the upper endplate (Figure 10E,F,G & H).

Table 7: The comparison of stress and displacement of internal fixation system in severe osteoporosis.

Severe Osteoporosis	OPS	DPS	CBS	EPS
Maximum stress of nail rod (Mpa)	165.21	161.58	170.82	153.56
Maximum displacement of nail rod (mm)	1.2944	1.2639	1.5148	1.2207
Maximum body stress (Mpa)	24.27	20.63	30.81	20.05
Maximum vertebral displacement (mm)	1.6612	1.6161	1.6625	1.5641

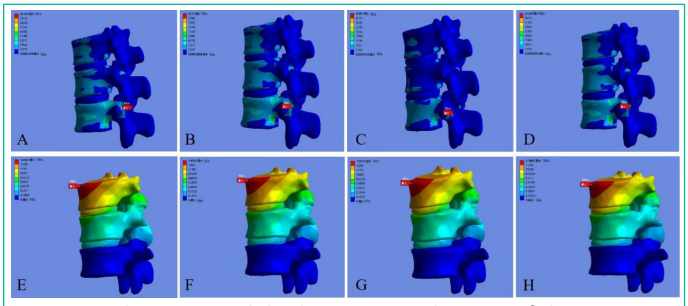

Figure 8: The stress and displacement nephogram of the posterior vertebral body of the pedicle nail in bone fixation systems, A: The stress cloud image of the Ordinary Pedicle Screws (OPS) model vertebral body; B: The stress cloud image of the Double-threaded Pedicle Screw (DPS) model vertebral body; C: The stress cloud image of the Cortical Bone track Screw (CBS) model vertebral body; D: The stress cloud image of the Expansive Pedicle Screw (EPS) model vertebral body; E: The displacement cloud image of the Ordinary Pedicle Screws (OPS) model vertebral body; F: The displacement cloud image of the Double-threaded Pedicle Screw (DPS) model vertebral body; G: The displacement cloud image of the Cortical Bone track Screw (CBS) model vertebral body; H: The displacement cloud image of the Expansive Pedicle Screw (EPS) model vertebral body.

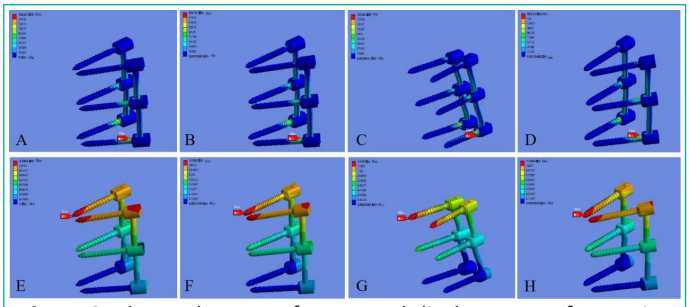

Figure 9: The nephogram of stress and displacement of posterior screws in mild osteoporosis pedicle nails, A: The stress nephogram of the Ordinary Pedicle Screws (OPS) model screw; B: The stress nephogram of the Double-threaded Pedicle Screw (DPS) model screw; C: The stress nephogram of the Cortical Bone track Screw (CBS) model screw; D: The stress nephogram of the Expansive Pedicle Screw (EPS) model screw; E: The displacement cloud image of the Ordinary Pedicle Screws (OPS) model screw; F: The displacement cloud image of the Double-threaded Pedicle Screw (DPS) model screw; G: The displacement cloud image of the Cortical Bone track Screw (CBS) model screw; H: The displacement cloud image of the Expansive Pedicle Screw (EPS) model screw.

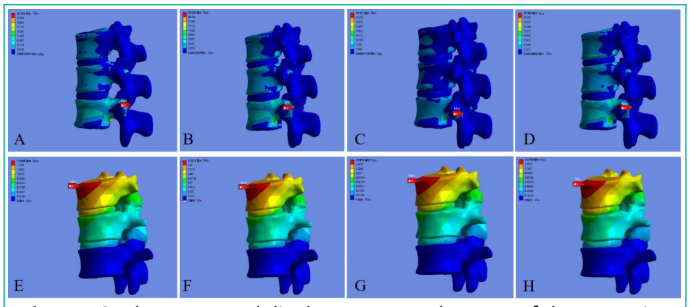

Figure 10: The stress and displacement nephogram of the posterior vertebral body of the pedicle nail in mild osteoporosis, A: The stress cloud image of the Ordinary Pedicle Screws (OPS) model vertebral body; B: The stress cloud image of the Double-threaded Pedicle Screw (DPS) model vertebral body; C: The stress cloud image of the Cortical Bone track Screw (CBS) model vertebral body; D: The stress cloud image of the Expansive Pedicle Screw (EPS) model vertebral body; E: The displacement cloud image of the Ordinary Pedicle Screws (OPS) model vertebral body; F: The displacement cloud image of the Double-threaded Pedicle Screw (DPS) model vertebral body; G: The displacement cloud image of the Cortical Bone track Screw (CBS) model vertebral body; H: The displacement cloud image of the Expansive Pedicle Screw (EPS) model vertebral body.

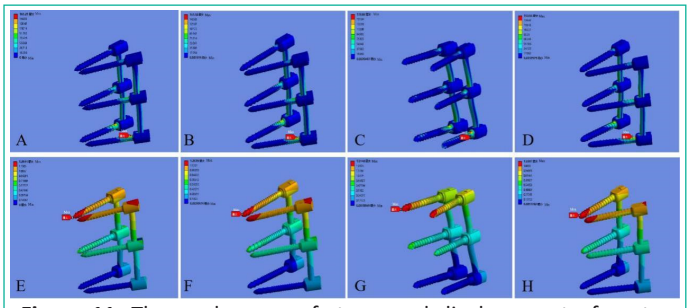

Figure 11: The nephogram of stress and displacement of posterior screws in in severe osteoporosis pedicle nails, A: The stress nephogram of the Ordinary Pedicle Screws (OPS) model screw; B: The stress nephogram of the Double-threaded Pedicle Screw (DPS) model screw; C: The stress nephogram of the Cortical Bone track Screw (CBS) model screw; D: The stress nephogram of the Expansive Pedicle Screw (EPS) model screw; E: The displacement cloud image of the Ordinary Pedicle Screws (OPS) model screw; F: The displacement cloud image of the Double-threaded Pedicle Screw (DPS) model screw; G: The displacement cloud image of the Cortical Bone track Screw (CBS) model screw; H: The displacement cloud image of the Expansive Pedicle Screw (EPS) model screw.

The Comparison of Stress and Displacement of Internal Fixation System in Severe Osteoporosis

In severe osteoporotic bone (65% cortical bone, 35% cancellous bone), the maximum stresses of OPS, DPS, CBS, and EPS were 165.21 Mpa, 161.58 Mpa, 170.82 Mpa, and 153.56 Mpa, respectively. The maximum displacements of screw rod were 1.2944 mm, 1.2639 mm, 1.4150 mm and 1.2207mm, respectively. The maximum vertebral stresses were 24.27 Mpa, 20.63 Mpa, 30.81 Mpa and 20.05 Mpa, respectively. The maximum vertebral displacements were 1.6612 mm, 1.6161 mm, 1.6625 mm and 1.5641 mm, respectively. Among them, CBS had the highest screw rod maximum stress, maximum displacement, maximum vertebral body stress, and maximum vertebral body displacement, while EPS had the lowest maximum stress and maximum displacement, as shown in Table 7.

The stress distribution cloud diagram of the screw showed that the stress distribution of the screw rod of the OPS and CBS model was relatively concentrated, mainly concentrated in the roots of the two lower fixed screws and the cross-linked rod (Figure 11A & C). The stress distribution of the screw rod of the DPS model and EPS model was relatively scattered, and the two screws fixed below shared part of the stress, and the stress distribution on the whole rod was relatively uniform (Figure 11B & D). The distribution cloud diagram of screw displacement showed that the displacement of OPS, DPS, and EPS models mainly occurred at the top of the two screws fixed above, the root of the screw, and the cross-linked rod (Figure 11E,F & H). The displacement of the CBS model occurred mainly at the top of the two screws fixed above (Figure 11G).

The stress distribution nephogram of the vertebral body showed that the stress in the vertebral body of the OPS, DPS, and CBS models were mainly concentrated in the lower end plate and the middle column (Figure 12A,B, & C). The stress of the vertebral body in the EPS model was mainly concentrated in the middle column (Figure 12D). Compared with the stress distribution transferred to the upper endplate, the stress distribution in the upper endplate of the OPS model, DPS model, and EPS model was the most dispersed (Figure 12B & D). The stress distribution in the upper endplate of the OPS model was scattered (Figure 12A). The stress distribution in the upper endplate was concentrated in the CBS model (Figure 12C). The distribution cloud map of vertebral body displacement showed that vertebral body displacement occurred at the upper endplate (Figure 12E,F,G & H).

Conclusion

In this study, we compared the mechanical differences among the OPS, DPS, CBS, and EPS models through finite element simulation mechanical analysis. The results showed that in the normal bone model (cortical bone 100%, cancellous bone 100%), the stress distribution of the EPS model was more dispersed, and the maximum stress and displacement of the screws and vertebral body were smaller than those of other screw models, indicating that the risk of fracture of the EPS model was lower than that of other screw models. In the reduced bone (cortical 85%, cancellous 85%) models, DPS and EPS models, the stress distribution of internal fixation was scattered, but the EPS model had the lowest maximum stress and displacement of screws and vertebral body. In the mild osteoporosis models (cortical 75%, cancellous 65%), DPS and EPS models, the stress distribution of the internal fixation was dispersed, but the maximum stress and displacement of the screws in the EPS model

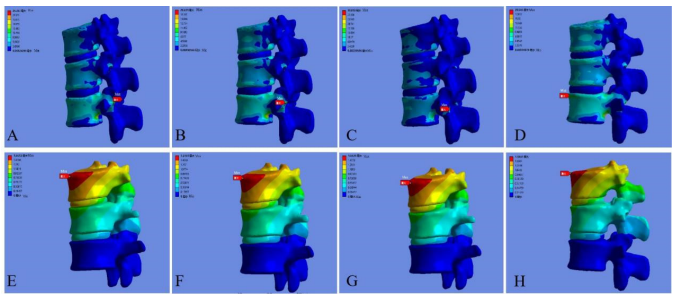

Figure 12: The stress and displacement nephogram of the posterior vertebral body of the pedicle nail in severe osteoporosis, A: The stress cloud image of the Ordinary Pedicle Screws (OPS) model vertebral body; B: The stress cloud image of the Double-threaded Pedicle Screw (DPS) model vertebral body; C: The stress cloud image of the Cortical Bone track Screw (CBS) model vertebral body; D: The stress cloud image of the Expansive Pedicle Screw (EPS) model vertebral body; E: The displacement cloud image of the Ordinary Pedicle Screws (OPS) model vertebral body; F: The displacement cloud image of the Double-threaded Pedicle Screw (DPS) model vertebral body; G: The displacement cloud image of the Cortical Bone track Screw (CBS) model vertebral body; H: The displacement cloud image of the Expansive Pedicle Screw (EPS) model vertebral body.

were smaller. In the severe osteoporosis model (65% cortical and 35% cancellous), DPS and EPS models, the stress distribution of the internal fixation was dispersed, but the maximum stress of the screws and the displacement of the vertebral body were smaller in the EPS model. Therefore, the spine stability of EPS model internal fixation system is stronger in osteoporosis treatment. Through the study and comparison, we believe that the EPS model has obvious mechanical advantages over others, making the spine more stable and the stress more dispersed. This may be related to the diameter of the screw, the design of the screw (cylindrical and conical), and the method of pedicle screw placement.

It has been shown that an increase in screw diameter of 1mm and an increase in screw length can significantly increase the screw insertion torque [9,10]. When the screw diameter increased by 0.5mm, the screw length increased by 5mm, and the screw length and diameter increased by 5mm and 0.5mm, the pull-out force increased by 15%, 33% and 49%, respectively [11,12]. However, some studies have shown that increasing the diameter and length of screws has limited effect on the fixation of augmented screws in osteoporotic vertebral bodies. The effect of increasing screw diameter and length on fixation strength was studied on human cadaver lumbar specimens of OP and non-OP. The results showed that increasing screw length could effectively improve fixation stiffness when the screw cross-sectional area was more than 70% of the pedicle cross-sectional area in non-OP specimens, and increasing screw diameter could effectively improve fixation stiffness when the insertion depth was more than 80% of the vertebral body. In the OP group, increasing the screw diameter or length had no significant effect on increasing the fixation stiffness [13,14]. In osteoporosis patients with BMD<0.7g/cm^2, the incidence of pedicle fracture was 41.2% when screw diameter exceeded 70% of the pedicle cross-sectional area [15,16].

The comparative study of biomechanical stability of cylindrical screws and conical screws is still controversial. Experiments on human cadaveric spinal specimens show that conical screws can increase the driving torque, while cylindrical screws have no such effect, but there is no difference in axial pulling strength between them [17. When the pedicle screws were inserted inwardly, the conical screws could significantly increase the extraction force and mechanical strength of the fixing system, and this enhancement effect was more obvious when the two pedicle screws were inserted inwardly to form a triangular structure. Compared with cylindrical screws, conical screws can effectively improve both bending strength and pulling force [18,19]. EPS is a new type of pedicle screw design, which can expand the front end of the screw and make the front end of the screw larger [20]. In vitro biomechanical tests on fresh calf lumbar vertebrae showed that EPS had significant differences in maximum extrusions moment (Tmax), maximum axial withdrawal force (Fmax) and maximum axial withdrawal force after revision compared with the three control screws (USS, Tenor, CDH screws) [21].

The inaccurate insertion point and poor placement of screws during the operation may cause the strength of the fixing system to decrease or fail. As for intraoperative positioning, a large number of anatomical studies have been conducted by domestic and foreign scholars. The classical literature suggests that the insertion point of pedicle screws should be the intersection of the middle line of the facet joint and the bisecting line of the transverse process. The researchers proposed that the apex of the lumbar spine with the "herringbone ridge" is located at or near the center of the pedicle, and is not affected by factors such as articular process hyperplasia or transverse process fracture [22]. Clinical application has proved that nail placement is more accurate, and it is the most commonly used method in lumbar pedicle screw surgery. Therefore, we believe that the spinal stability and stress distribution caused by pedicle screw placement in the spine are closely related to the screw diameter, screw design (column and cone), and the method of pedicle screw placement. In a short, the results of finite element analysis show that the expandable pedicle screw internal fixation system may have mechanical advantages over the traditional internal fixation system in the treatment of vertebral fractures caused by osteoporosis, and it can provide sufficient mechanical stability at the fracture end, which is worthy of further promotion and application.

Author Statements

Conflict of Interest

The authors have no financial disclosures or other conflicts of interest to report related to the content of this article.

References

1. Yong EL, Logan S. Menopausal osteoporosis: screening, prevention and treatment. Singapore Medical Journal. 2021; 62: 159-166.

2. Ma YZ, Wang YP, Liu Q, et al. Chinese Guidelines for the diagnosis and treatment of osteoporosis in the elderly (2018). Chinese Journal of Gerontology. 2019; 39: 2557-2575.

3. Hirai T, Uehara M, Miyagi M, Takahashi S, Nakashima H. Current Advances in Spinal Diseases of the Elderly: Introduction to the Special Issue. Journal of Clinical Medicine. 2021; 10: 3298.

4. D'antoni F, Russo F, Ambrosio L, Bacco L, Vollero L, Vadala G, et al. Artificial Intelligence and Computer Aided Diagnosis in Chronic Low Back Pain: A Systematic Review. International Journal of Environmental Research and Public Health. 2022; 19: 5971.

5. Johannesdottir F, Allaire B, Bouxsein ML. Fracture Prediction by Computed Tomography and Finite Element Analysis: Current and Future Perspectives. Current Osteoporosis Reports. 2018; 16: 411-422.

6. Meslier QA, Shefelbine SJ. Using Finite Element Modeling in Bone Mechanoadaptation. Current Osteoporosis Reports. 2023; 21: 105-116.

7. Shekouhi N, Kellkar A, Dick D, Goel VK, Shaw D. Current bench-top protocols are not appropriate for the evaluation of distraction-based growing rods: a literature review to justify a new protocol and its development. Eur Spine J. 2022; 31: 963-979.

8. Guo H, Li J, Gao Y, Nie S, Quan C, Li J, et al. A Finite Element Study on the Treatment of Thoracolumbar Fracture with a New Spinal Fixation System. BioMed Research International. 2021; 2021: 1-9.

9. Lea MA, Elmalky M, Sabou S, Sabou S, Siddique I, Verma R, et al. Revision pedicle screws with impaction bone grafting: a case series. Journal of Spine Surgery. 2021; 7: 344-353.

10. Matsukawa K, Yato Y, Imabayashi H. Impact of Screw Diameter and Length on Pedicle Screw Fixation Strength in Osteoporotic Vertebrae: A Finite Element Analysis. Asian Spine Journal. 2021; 15: 566-574.

11. Viezens L, Sellenschloh K, Puschel K, Morlock MM, Lehmann W, Huber G, et al. Impact of Screw Diameter on Pedicle Screw Fatigue Strength—A Biomechanical Evaluation. World Neurosurgery. 2021; 152: e369-e376.

12. Lai DM, Shih YT, Chen YH, Chien A, Wang JL. Effect of pedicle screw diameter on screw fixation efficacy in human osteoporotic thoracic vertebrae. Journal of Biomechanics. 2018; 70: 196-203.

13. Brantley AG, Mayfield JK, Koeneman JB, Clark KR. The effects of pedicle screw fit: an in vitro study. Spine. 1994; 19: 1752-1758.

14. Jazini E, Petraglia C, Moldavsky M, Tannous O, Weir T, Saifi C, et al. Finding the right fit: studying the biomechanics of undertapping with varying thread depths and pitches [J]. The Spine Journal. 2017; 17: 574-578.

15. Plais N, Mengis C, Gallego Bustos JM, Tome-Bermejo F, Peiro-Garcia A, Buitrago AN, et al. Simplified Pedicle Subtraction Osteotomy for Osteoporotic Vertebral Fractures. International Journal of Spine Surgery. 2021; 15: 1004-1013.

16. Hirano T, Hasegawa K, Washio T, Hara T, Takahashi H. Fracture risk during pedicle screw insertion in osteoporotic spine. J Spinal Disord. 1998; 11: 493-497.

17. Moran JM, Liu MY, Tsai TT, Lai PL, Hsieh MK, Chen LH, et al. Biomechanical comparison of pedicle screw fixation strength in synthetic bones: Effects of screw shape, core/thread profile and cement augmentation. Plos One. 2020; 15: e0229328.

18. Amaritsakul Y, Chhao CK, Lin J. Comparison study of the pull-out strength of conventional spinal pedicle screws and a novel design in full and backed-out insertions using mechanical tests. Proc Inst Mech Eng H. 2014; 228: 250-257.

19. Amaritsakul Y, Chao CK, Lin J. Biomechanical evaluation of bending strength of spinal pedicle screws, including cylindrical, conical, dual core and double dual core designs using numerical simulations and mechanical tests. Medical Engineering & Physics. 2014; 36: 1218-1223.

20. Williams BO, Tai CL, Tsai TT, Lai PL, Chen YL, Liu MY, et al. A Biomechanical Comparison of Expansive Pedicle Screws for Severe Osteoporosis: The Effects of Screw Design and Cement Augmentation. Plos One. 2015; 10: e0146294.

21. Esenkaya I, Denizhan Y, Kaygusuz MA, Yetmez M, Kelestemur MH. Comparison of the pull-out strengths of three different screws in pedicular screw revisions: a biomechanical study. Acta Orthop Traumatol Turc. 2006; 40: 72-81.

22. Zhou LP, Zhang RJ, Jiang ZF, Tao EX, Shang J, Shen CL, et al. Ideal entry point and trajectory for C2 pedicle screw placement in basilar invagination patients with high-riding vertebral artery based on 3D computed tomography. Spine J. 2022; 22: 1281-1291.